# Supporting Information

**Metal(II)-induced synthesis asymmetric fluorescence benzimidazoles complexes and their dye-sensitized solar cells performance as co-sensitizers**

**Xinming Wang,**[†,‡] **Ruiqing Fan,**[*, †] **Yuwei Dong,**[†] **Ting Su,**[†] **Jian Huang,**[†] **Xi Du,**[†] **Ping Wang,**[†] **Yulin Yang,**[*, †]

[†]*MIIT Key Laboratory of Critical Materials Technology for New Energy Conversion and Storage, School of Chemistry and Chemical Engineering, Harbin Institute of Technology, Harbin 150001, P. R. of China*

[‡]*Department of Chemistry, Harbin University of Science And Technology, Harbin 150080, P. R. China*

# Index

**Materials and General Methods**

All solvents and chemicals used in synthesis and analysis were commercially available and used as received without further purifiion. IR spectra were recorded on a Nicolet impact 410 FT-IR spectrometer in the range of 4000-400 cm$^{-1}$ as KBr pellets. $^1$H NMR spectra were recorded on a Bruker ACF spectrometer at 400 MHz in CD$_3$CN solvent at room temperature. $^{13}$C NMR (150 MHz) spectra were recorded on a Bruker Avance-600 spectrometer in CD$_3$CN. A THERMO Finnigan LCQ Advantage Max ion trap mass spectrometer was used to collect ESI–MS spectra. Chemical shifts (δ) were reported in part per million (ppm) relative to an internal standard of TMS. The melting points were determined using a capillary melting point apparatus and are uncorrected. Powder X–ray diffraction (PXRD) patterns were recorded in the 2θ range of 5–50° using Cu Kα radiation by Shimadzu XRD–6000 X–ray Diffractometer. Elemental analyses for carbon, hydrogen, and nitrogen were carried out on a Perkin-Elmer 240c element analyzer. UV-Vis spectra were obtained on a Perkin-Elmer Lambda 20 spectrometer. The photoluminescence measurements were carried out on an Edinburgh FLS920 fluorescence spectrometer equipped with a peltier-cooled Hamamatsu R928 photo multiplayer tube. Lifetime studies were performed using photon-counting system with a microsecond pulse lamp as the excitation source. Data were analyzed using the nonlinear least squares procedure in combination with an iterative convolution method. The decay curve is well fitted into a double exponential function: $I = I_0 + A_1 \exp(-t/\tau_1) + A_2 \exp(-t/\tau_2)$, where $I$ and $I_0$ are the luminescent intensities at time $t = $ t and $t = 0$, respectively, whereas $\tau_1$ and $\tau_2$ are defined as the luminescent lifetimes. The average lifetime $<\tau>$ was calculated according to the following equation (1):

$$<\tau> = \frac{\tau_1^2 A_1\% + \tau_2^2 A_2\%}{\tau_1 A_1\% + \tau_2 A_2\%}$$ (1). The luminescence quantum yields were measured in

CH$_3$CN at room temperature and cited relative to a reference solution of quinine sulfate ($\Phi = 0.546$ in 0.5 mol dm$^{-3}$ H$_2$SO$_4$) as a standard for blue and green luminescence complexes, and they were calculated according to the well−known

equation (2) [1]: $$\frac{\varphi_{overall}}{\varphi_{ref}} = \left(\frac{n}{n_{ref}}\right)^2 \frac{A_{ref}}{A} \frac{I}{I_{ref}}$$ (2). In equation (2), $n$, $A$, and $I$ denote the

refractive index of solvent, the area of the emission spectrum, and the absorbance at the excitation wavelength, respectively, and $\varphi_{ref}$ represents the quantum yield of the standard solution. The subscript *ref* denotes the reference, and the absence of a subscript implies an unknown sample. For the determination of the quantum yield, the

absorbance was kept in the range of 0.05–0.1 to avoid the interference of reabsorption. Cyclic voltammetry (CV) were performed with an electrochemical workstation (CHI660d, Chenhua, Shanghai) using a three-electrode cell with a Pt working electrode, a Pt wire auxiliary electrode, and a saturated calomel reference electrode in saturated KCl solution. The supporting electrolyte was 0.1 M tetrabutyl ammonium hexafluoro phosphate ($TBAPF_6$, Fluka, electrochemical grade) in acetonitrile as the solvent. Photocurrent–photovoltage ($I$–$V$) curves were recorded on the Keithley model 2400 digital source meter using a mask with an aperture area of 0.16 $cm^{-2}$. The irradiance of AM 1.5 global sunlight from a filtered 500 W xenon lamp light source was set at 100 mW $cm^{-2}$ and was calibrated using a standard silicon solar cell (No. NIMMS1123, calibrated at the National Institute of Metrology, P. R. China). Based on the $I$–$V$ curve, the fill factor ($FF$) is defined as: $FF = (J_{max} \times V_{max})/(J_{sc} \times V_{oc})$, where $J_{max}$ and $V_{max}$ are the photocurrent density and photovoltage for the maximum power output; $J_{sc}$ and $V_{oc}$ are the short-circuit photocurrent density and open circuit photovoltage, respectively. The overall energy conversion efficiency $\eta$ is defined as: $\eta = (FF \times J_{sc} \times V_{oc})/P_{in}$ where $P_{in}$ is the power of the incident light. The incident photon-to-current conversion efficiency (IPCE) is measured on an EQE/IPCE spectral response system (Newport). Electrochemical impedance spectra (EIS) are recorded using the CHI660D Electrochemical Analyzer (Chenhua, China), and the measurements are taken over a frequency range of 0.1–100 kHz under standard global AM 1.5 solar irradiation or in the dark by applying a forward bias of −0.75 V.

**X-ray Diffraction Analysis**

For the Schiff base ligand **L**, complexes **1–4**, the suitable crystal were coated with hydrocarbon oil and attached to the tip of a glass fiber, which was the transferred to a Siemens SMART 1000 CCD diffractometer equipped with graphite-monochromated Mo Kα radiation (λ=0.71073 Å), operating at 298 ± 2 K. Details of the crystal parameters, data collection and refinement for the structure are collected in Table 1. After data collection, an empirical absorption correction was applied. And the structure was solved by conventional direct method and refined by full-matrix least squares based on $F^2$ using the SHELXTL 5.1 software package[2,3]. The hydrogen atoms were placed at calculated positions and refined as riding atoms with isotropic displacement parameters. All non-hydrogen atoms were refined anisotropically. The CCDC 1449510, 1449511, 1449512, 1449513 and 1449514 contain the crystallographic data of **L** and complex **1–4** in this paper. These data can be obtained free of charge at https://deposit.ccdc.cam.ac.uk/.

**Assembly of Dye-sensitized Solar Cells (DSSCs)**

The FTO conducting glass (fluorine-doped $SnO_2$, sheet resistance15 Ω per square, transmission 90% in the visible) was purchased from NSG, Japan, and cleaned by a

standard procedure. N719 [cis-bis(isothiocyanato)bis(2,2-bipyridyl-4,4-dicarboxylato)-ruthenium(II)bis-tetrabutylammonium] was purchased from Solaronix Company, Switzerland. DSSCs were fabricated using the following procedure. The $TiO_2$ paste was cast onto the FTO substrate by the screen-printing method, followed by drying at 100 ℃ for 5 min and this process was repeated six times, followed by sintering at 500 ℃ for 15 min in air to obtain a transparent $TiO_2$ photoelectrode with the thickness of *ca*. 10 μm. In this work, the DSSCs devices were assembled by sandwiching the electrolyte between the dye sensitized photoanode and the counter electrode. The complex and N719 co-sensitized photoanode were fabricated using the following procedure: firstly, we immersed the mesoporous $TiO_2$ photoelectrode into 0.3 mM complex solution in absolute ethanol for 2 h, and then washed it with ethanol and dried with a blower; Secondly, we further immersed the electrodes in a 0.3 mM N719 solution in absolute ethanol for 12 h, and then washed it with ethanol and dried with blower again. The single N719 sensitized photoanode was prepared by only immersing $TiO_2$ photoelectrode into a 0.3 mM N719 solution in absolute ethanol for 14 h taken as control group. The sandwich-type solar cell device was assembled by placing a platinum-coated conductive glass as counter electrode on the co-sensitized photoanode. The electrolyte used in this work was 0.5 M LiI + 0.05 M $I_2$ + 0.1 M tert-butyl pyridine in a 1:1 (volume ratio) of acetonitrile–propylene carbonate. The platinum counter electrode was prepared by depositing $H_2PtCl_6$ paste onto the FTO glass substrates and then sintering at 450 ℃ for 30 min. The cells were assembled by sandwiching the electrolyte between the dye sensitized photoanode and the counter electrode and the assembly were held together using mini-binder clips.
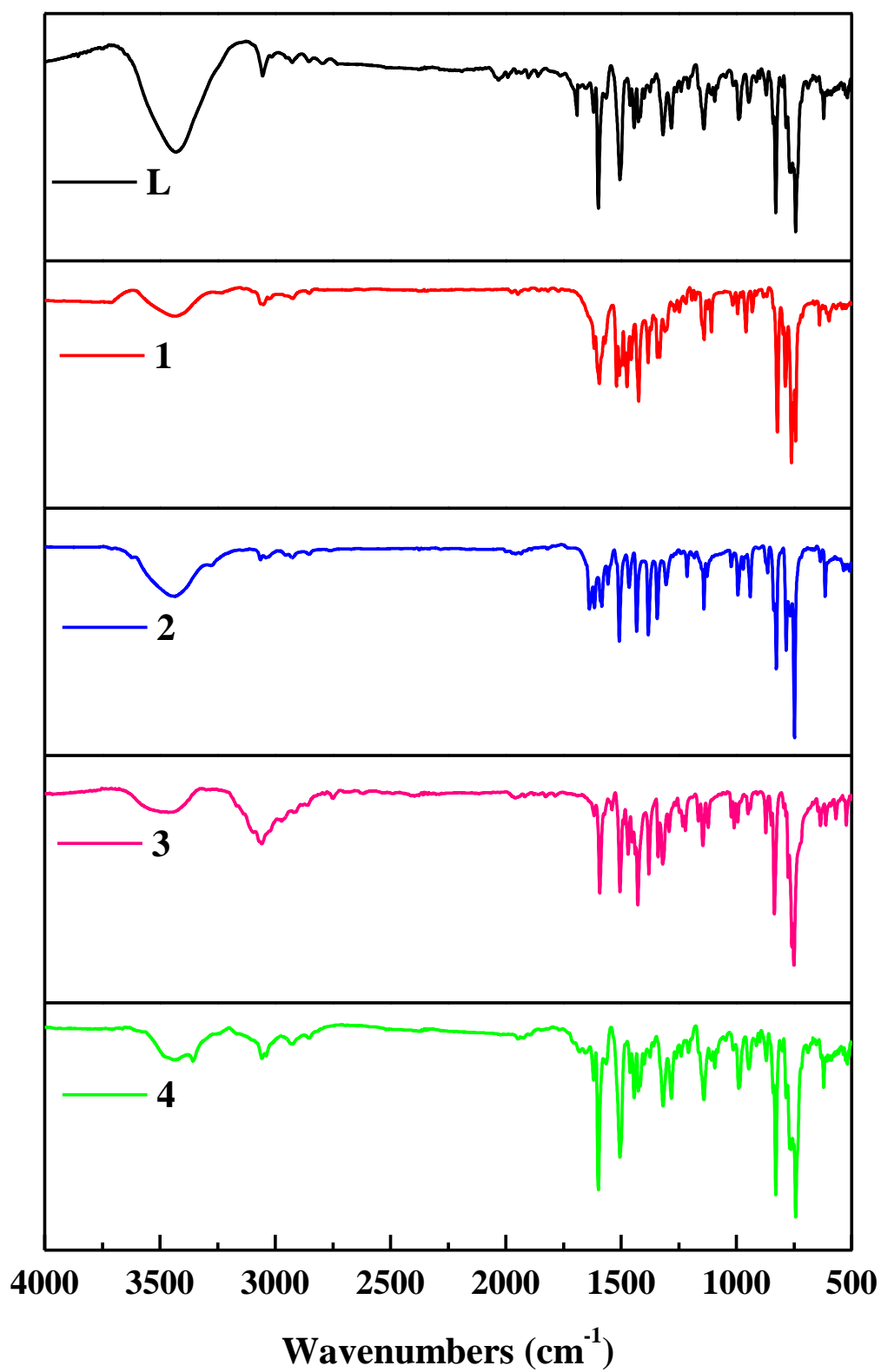
**Figure S1.** Infrared spectra of ligand **L** and complexes **1–4** recorded from a KBr pellet.
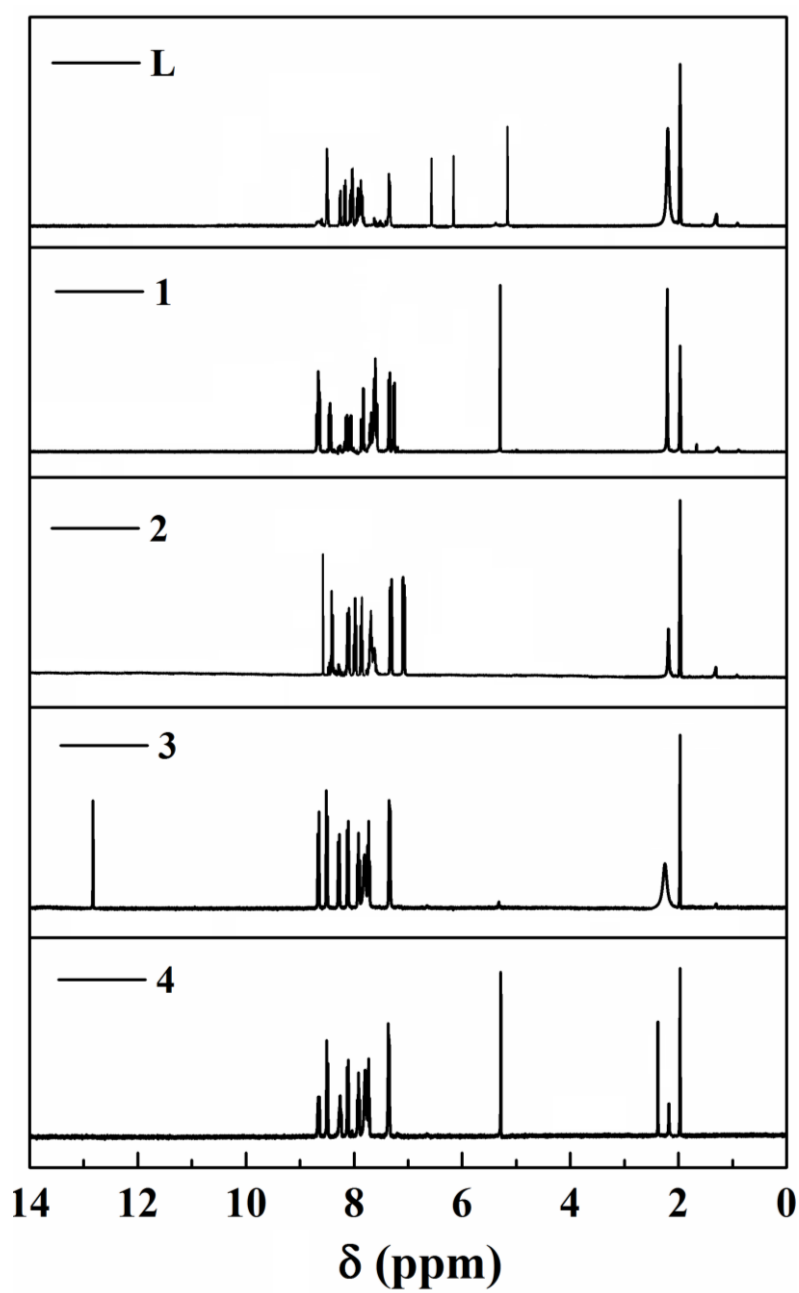
**Figure S2.** $^1$H NMR spectra of ligand **L** and complexes **1–4** in CD$_3$CN.
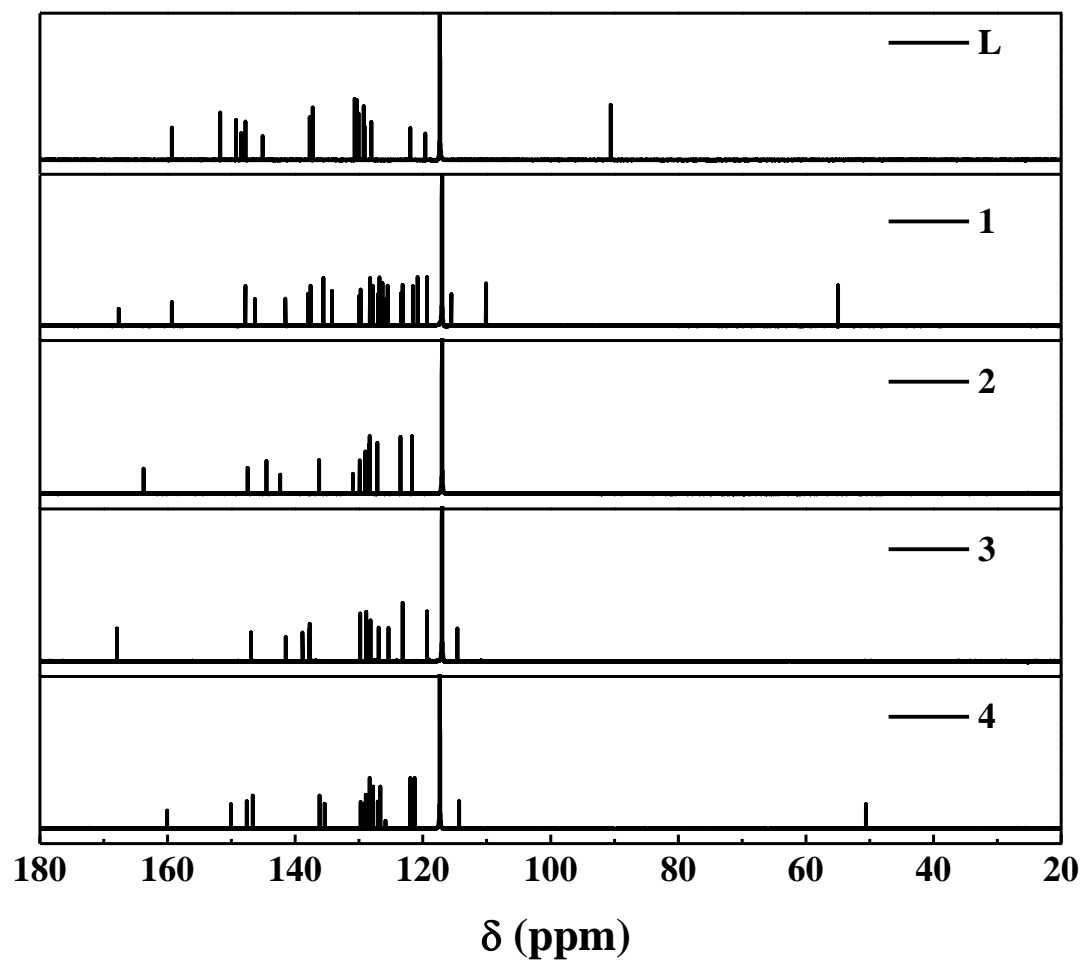
**Figure S3.** $^{13}$C NMR spectra of ligand **L** and complexes **1**–**4** in CD$_3$CN.
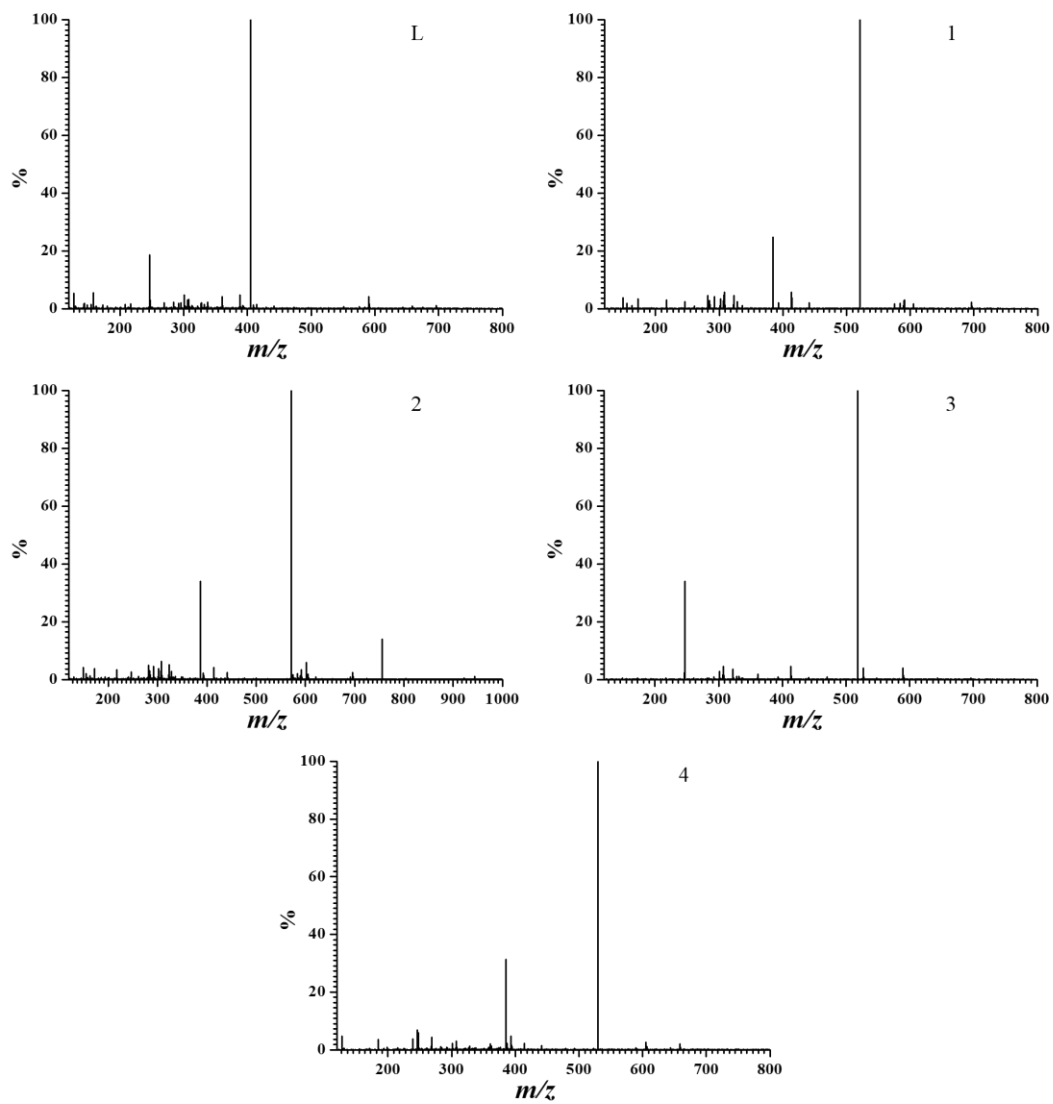
**Figure S4.** The ESI–MS spectra of **L** and complexes **1**–**4**.
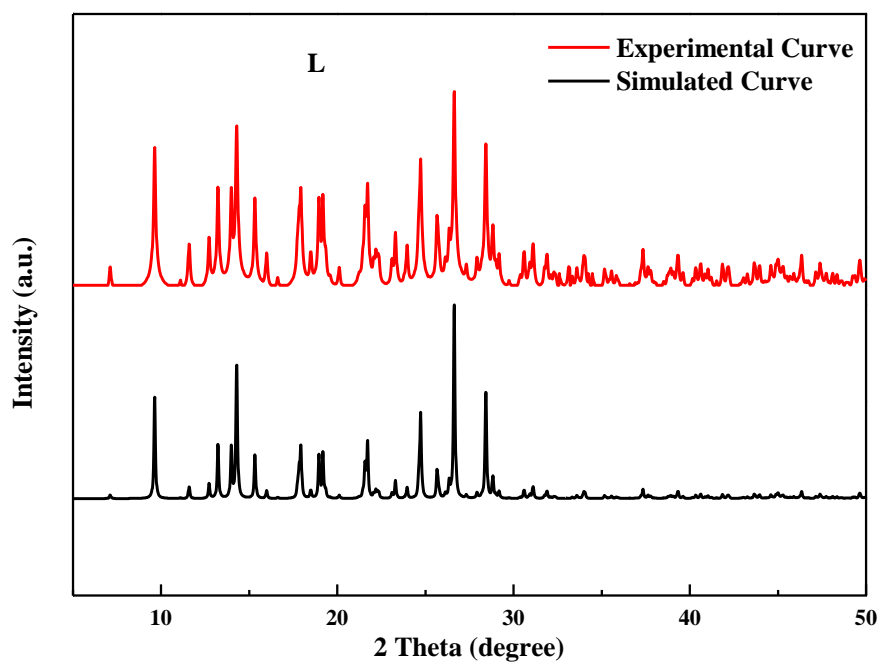
**Figure S5.** The PXRD contrast curves of Schiff base **L**.
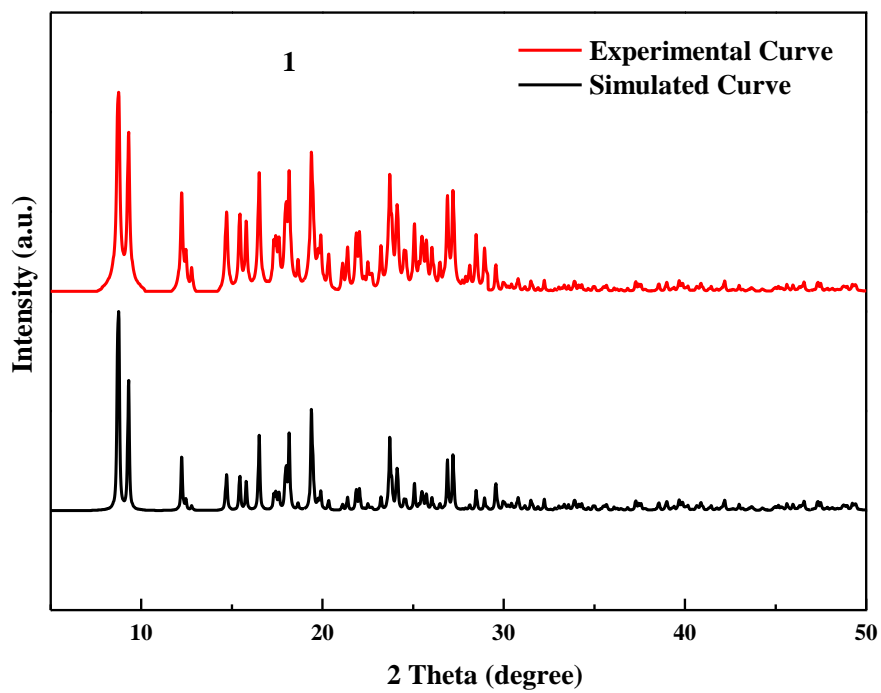


**Figure S6.** The PXRD contrast curves of complex **1**.
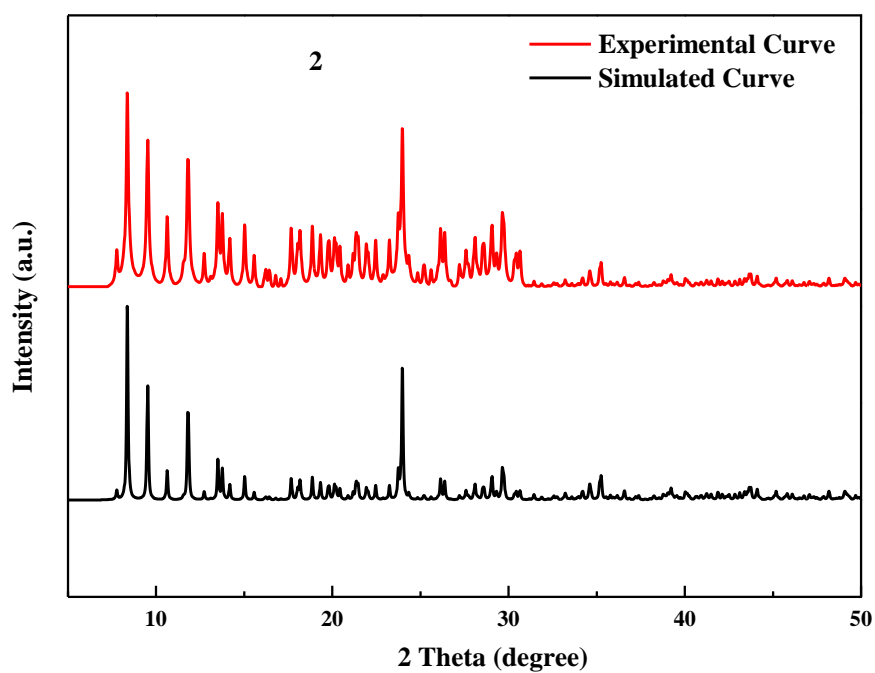
**Figure S7.** The PXRD contrast curves of complex **2**.
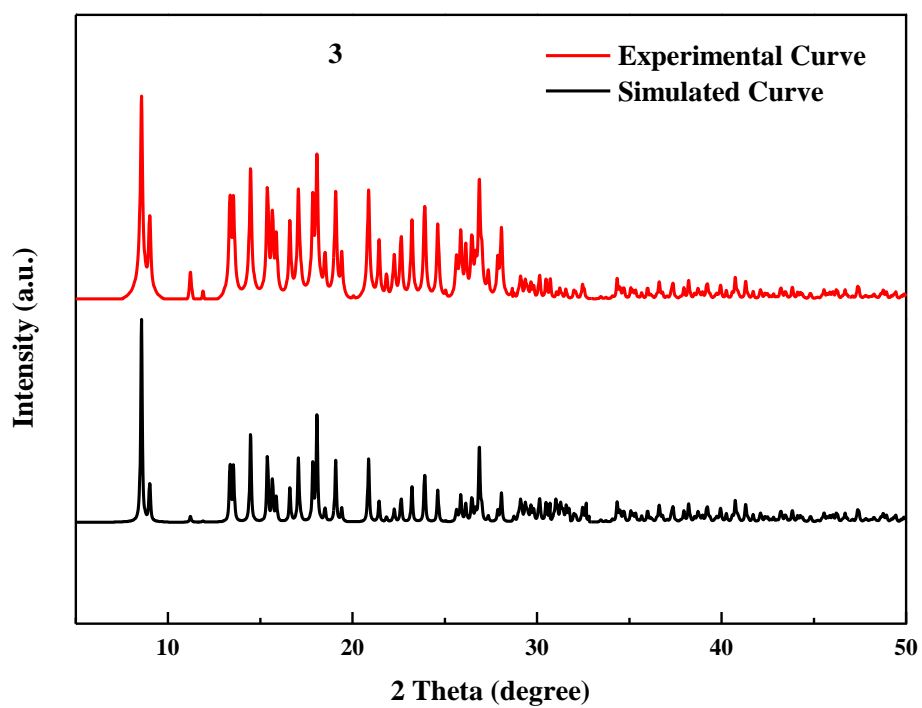


**Figure S8.** The PXRD contrast curves of complex **3**.
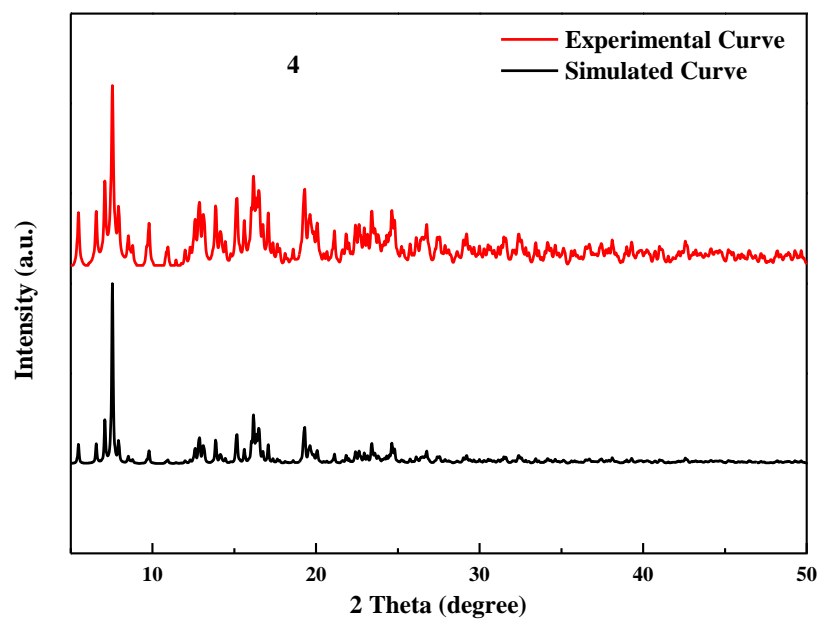
**Figure S9.** The PXRD contrast curves of complex **4**.
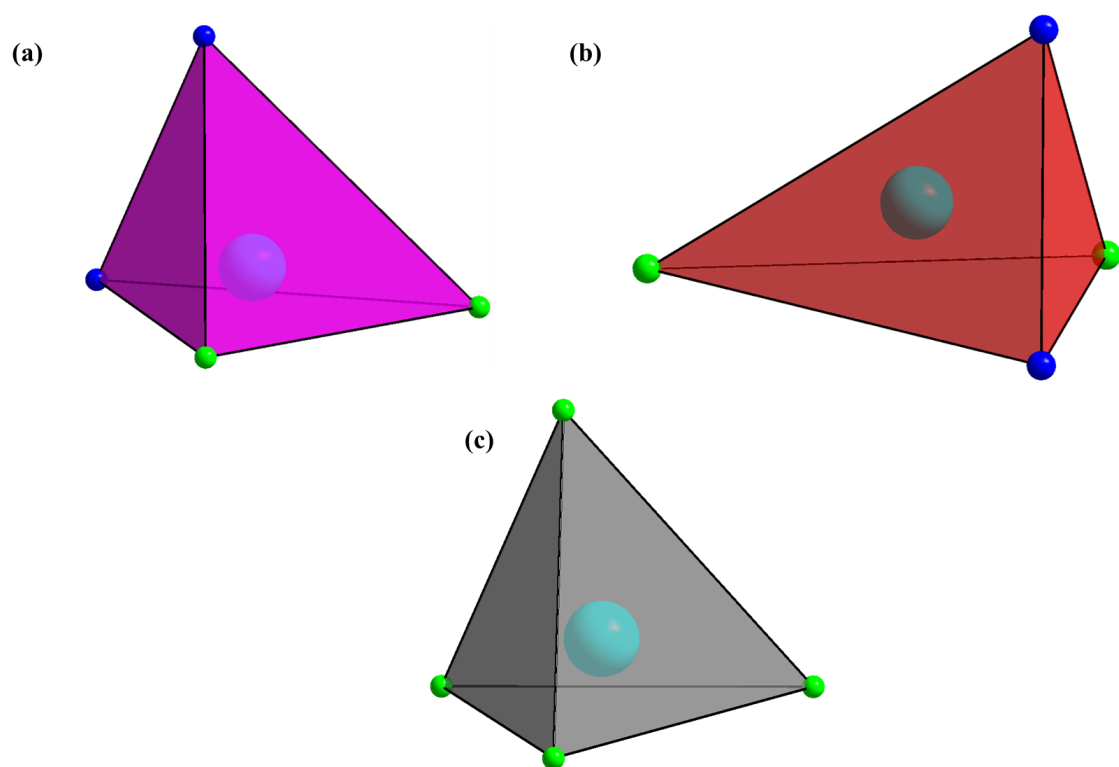
**Figure S10.** The coordinating polyhedron of **1** (a), **3** (b), **4** (c).



**Figure S11.** The luminescence decay curves of Schiff base **L** and complexes **1-4** in CH$_3$CN.

**Figure S12.** The luminescence decay curves of Schiff base **L** and complexes **1**-**4** in solid state.

**Table S1.** Selected bond lengths [Å] and angles [°] for **L**.

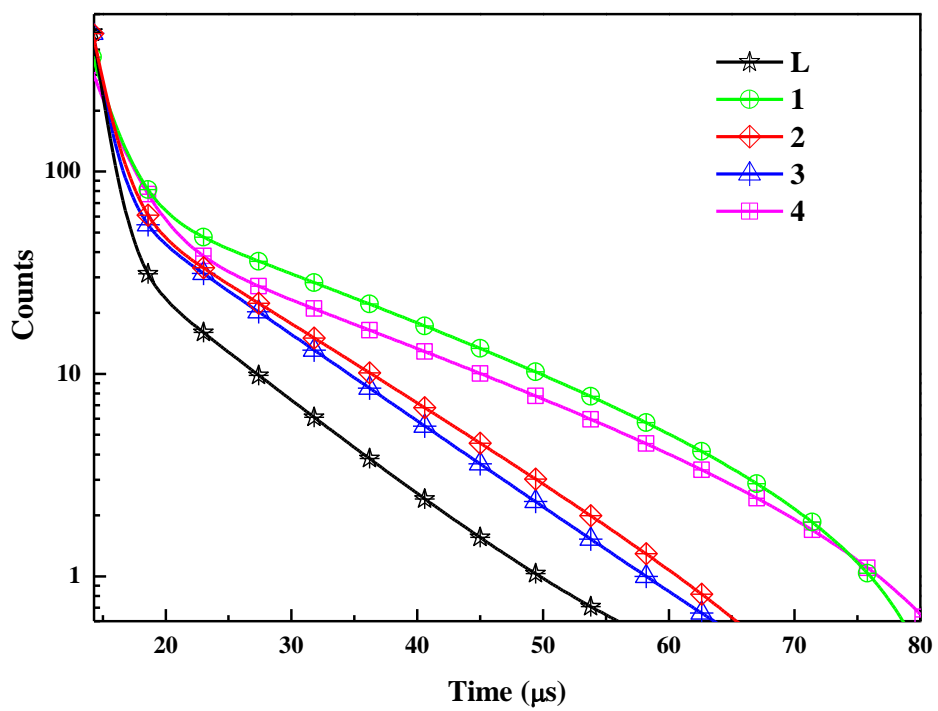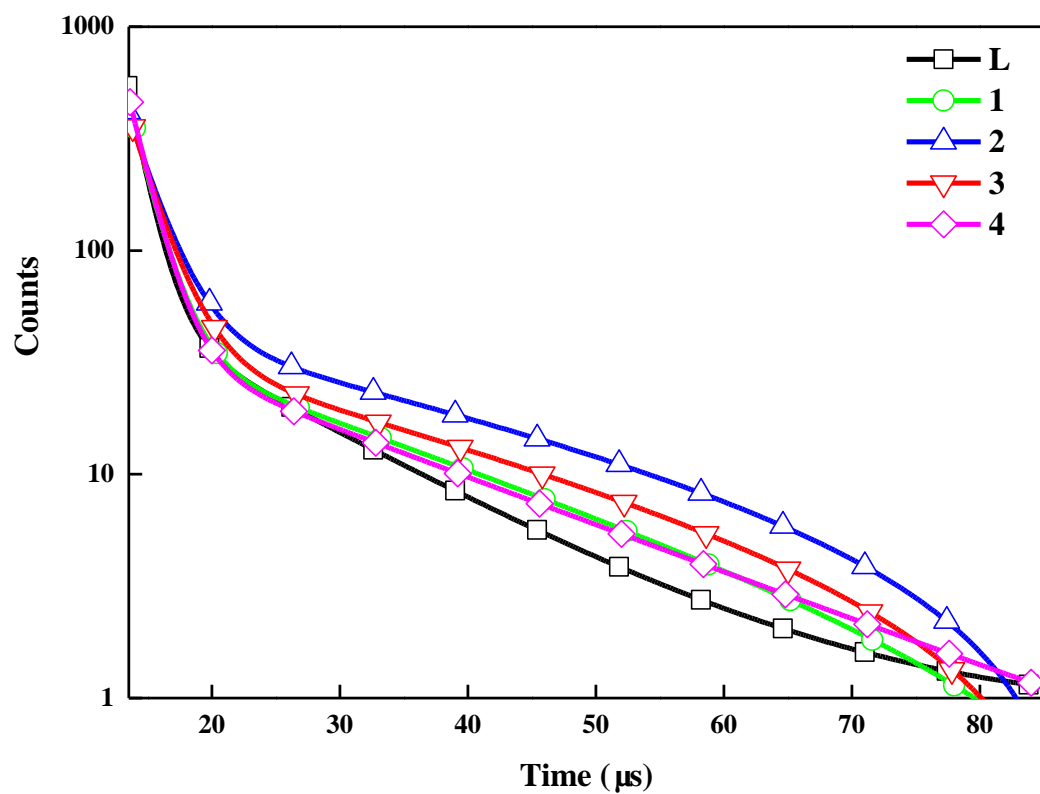| | | | | | |
|---|---|---|---|---|---|
| O(1)-C(10) | 1.219(4) | O(1)-H(1) | 0.8400 | N(1)-C(1) | 1.322(5) |
| N(1)-C(5) | 1.368(5) | N(2)-C(11) | 1.323(5) | N(2)-C(15) | 1.367(5) |
| N(3)-C(10) | 1.353(5) | N(3)-C(21) | 1.410(5) | N(3)-H(3A) | 0.8800 |
| N(4)-C(20) | 1.276(5) | N(4)-C(22) | 1.425(5) | C(1)-C(2) | 1.402(5) |
| C(10)-O(1)-H(1) | 109.5 | C(1)-N(1)-C(5) | 116.9(3) | C(11)-N(2)-C(15) | 117.7(3) |
| C(10)-N(3)-C(21) | 129.3(3) | C(10)-N(3)-H(3A) | 115.4 | C(21)-N(3)-H(3A) | 115.4 |
| C(20)-N(4)-C(22) | 119.8(4) | N(1)-C(1)-C(2) | 124.6(4) | N(1)-C(1)-C(10) | 116.7(3) |

**Table S2.** Initial Optimization

| entry | Metal salt | method[a] | complex | Yield (%)[b] |
|---|---|---|---|---|
| 1 | $ZnCl_2$ | A | **1** | 70.34 |
| 2 | $CdCl_2$ | A | —— | —— |
| 3 | $HgCl_2$ | A | —— | —— |
| 4 | $ZnCl_2$ | B | **1** | 35 |
| 5 | $CdCl_2$ | B | **2** | 75.21 |
| 6 | $HgCl_2$ | B | —— | —— |
| 7 | $ZnCl_2$ | C | **1** | Below 5 |
| 8 | $CdCl_2$ | C | **2** | 12.23 |
| 9 | $HgCl_2$ | C | **3** | 54.81 |

[a] Method A: Reactions maintained for 5 hours under refluxing at 80 ℃ with 1 equiv of $MCl_2$ and 1 equiv of **L** in the mixed solvent of methanol and toluene. Method B: 1 equiv of $MCl_2$ and 1 equiv of **L** were dissolved and heated in a sealed vial at 80 ℃ for 5 hours. Method C: A mixture of 1 equiv $MCl_2$ and 1 equiv **L** in the presence of a catalytic amount of triethylamine was dissolved in the mixed solvent, which was transferred into 8 mL sealed vial and heated at 100 ℃ for 5 hours.[b] Yields determined by $^1$H NMR spectroscopy with an internal standard (phenol).

**Table S3.** Selected bond lengths [Å] and angles [°] for **[Zn(L$^1$)Cl$_2$] (1)**.

| | | | | | |
|---|---|---|---|---|---|
| Zn(1)-N(2) | 2.017(2) | Zn(1)-N(1) | 2.102(2) | Zn(1)-Cl(1) | 2.196(8) |
| Zn(1)-Cl(2) | 2.212(8) | N(1)-C(1) | 1.330(3) | N(1)-C(5) | 1.370(3) |
| N(2)-C(10) | 1.326(3) | N(2)-C(11) | 1.385(3) | N(3)-C(10) | 1.364(3) |
| N(3)-C(16) | 1.389(3) | N(3)-C(17) | 1.455(3) | N(4)-C(18) | 1.308(3) |
| N(2)-Zn(1)-N(1) | 79.63(8) | N(2)-Zn(1)-Cl(1) | 121.08(6) | N(1)-Zn(1)-Cl(1) | 115.48(6) |
| N(2)-Zn(1)-Cl(2) | 109.15(6) | N(1)-Zn(1)-Cl(2) | 117.76(3) | Cl(1)-Zn(1)-Cl(2) | 117.96(3) |
| C(1)-N(1)-Zn(1) | 113.38(1) | C(5)-N(1)-Zn(1) | 126.04(1) | C(11)-N(2)-Zn(1) | 138.31(1) |

**Table S4.** Selected bond lengths [Å] and angles [ °] for **[Cd(L²)Cl₂] (2)**.

| | | | | | |
|---|---|---|---|---|---|
| Cd(1)-N(4) | 2.322(6) | Cd(1)-N(2) | 2.348(6) | Cd(1)-N(1) | 2.406(5) |
| Cd(1)-N(3) | 2.418(5) | Cd(1)-Cl(2) | 2.605(2) | Cd(1)-Cl(1) | 2.616(2) |
| Cd(2)-Cl(3) | 2.380(2) | Cd(2)-Cl(4) | 2.434(2) | Cd(2)-Cl(2) | 2.522(2) |
| Cd(2)-Cl(1) | 2.529(2) | | | | |

| | | | | | |
|---|---|---|---|---|---|
| N(4)-Cd(1)-N(2) | 69.5(2) | N(4)-Cd(1)-N(1) | 138.9(2) | N(2)-Cd(1)-N(1) | 69.4(2) |
| N(4)-Cd(1)-N(3) | 70.6(2) | N(2)-Cd(1)-N(3) | 140.1(2) | N(1)-Cd(1)-N(3) | 150.4(2) |
| N(4)-Cd(1)-Cl(2) | 104.05(1) | N(2)-Cd(1)-Cl(2) | 99.50(16) | N(1)-Cd(1)-Cl(2) | 84.18(14) |
| N(3)-Cd(1)-C l (2) | 87.82(14) | N(4)-Cd(1)-Cl(1) | 103.35(1) | N(2)-Cd(1)-Cl(1) | 108.85(1) |
| N(1)-Cd(1)-Cl(1) | 88.33(14) | N(3)-Cd(1)-Cl(1) | 82.51(14) | Cl(2)-Cd(1)-Cl(1) | 145.91(7) |
| Cl(3)-Cd(2)-Cl(4) | 117.01(8) | Cl(3)-Cd(2)-Cl(2) | 110.49(8) | Cl(4)-Cd(2)-Cl(2) | 106.53(7) |
| Cl(3)-Cd(2)-Cl(1) | 109.13(9) | Cl(4-)Cd(2)-Cl(1) | 107.25(7) | Cl(2)-Cd(2)-Cl (1) | 105.81(7) |
| Cd(2)-Cl(1)-Cd(1) | 105.17(7) | Cd(2)-Cl(2)-Cd(1) | 116.60(7) | | |

**Table S5.** Selected bond lengths [Å] and angles [ °] for **[Hg(L³)Cl₂] (3)**.

| | | | | | |
|---|---|---|---|---|---|
| Hg(1)-N(2) | 2.228(4) | Hg(1)- N(1) | 2.448(4) | Hg(1)-Cl(1) | 2.342(1) |
| Hg(1)-Cl(2) | 2.488(1) | N(3)-C (12) | 1.384(7) | N(1)-C (1) | 1.325(6) |

| | | | | | |
|---|---|---|---|---|---|
| N(2)- Hg(1)-Cl(1) | 137.94(1) | N(2)-Hg(1)-N(1) | 72.17(1) | N(1)-Hg(1)-Cl(1) | 117.18(1) |
| N(2)- Hg(1)-Cl(2) | 107.14(1) | Cl(1)- Hg (1)-Cl(2) | 110.05(6) | N(1)- Hg (1)-Cl(2) | 102.14(1) |
| C(1)-N(1)-Hg(1) | 118.5(4) | C(1)-N(1)-Hg(1) | 113.2(3) | C(5)-N(1)- Hg(1) | 128.3(3) |
| C(10)-N(2)- Hg(1) | 116.2(3) | C(11)-N(2)- Hg(1) | 136.4(3) | C(10)-N(3)-C(12) | 107.8(4) |

**Table S6.** Selected bond lengths [Å] and angles [ °] for **(L⁴)₂(HgCl₄) (4)**.

| | | | | | |
|---|---|---|---|---|---|
| Hg(2)- Cl(1) | 2.470(2) | Hg(2)- Cl(2) | 2.435(2) | Hg(2)- Cl(3) | 2.481(2) |
| Hg(2)- Cl(4) | 2.517(2) | N(1)B-C(6)B | 1.379(9) | N(2)B-C (7)B | 1.370(9) |
| N(3)B-C(9)B | 1.310(9) | N(4)B-C(18)B | 1.287(10) | N(5)B-C(28)B | 1.313(10) |

| | | | | | |
|---|---|---|---|---|---|
| Cl(2)-Hg(2)-Cl(1) | 112.65(8) | Cl(2)-Hg(2)-Cl(3) | 115.04(9) | Cl(1)-Hg(2)-Cl(3) | 105.79(8) |
| Cl(2)-Hg(2)-Cl(4) | 107.86(7) | Cl(1)-Hg (2)-Cl(4) | 111.53(9) | Cl(3)-Hg(2)-Cl(4) | 103.66(6) |

**Table S7.** Photoluminescent Data for **L** and **1**–**4** in acetonitrile solution at 298 K

| Compound | Absorption $(\varepsilon)^a$ (nm, $dm^3mol^{-1}cm^{-1}$) | Excitation $(\lambda_{ex}, nm)$ | Emission $(\lambda_{max}, nm)$ | CIE 1931 (x, y) | $\tau_1$ (µs) | $\tau_2$ (µs) | $(\tau, µs)^b$ | $\Phi^{a,c}$ |
|---|---|---|---|---|---|---|---|---|
| **L** | 311 (69882), 356 (27778) | 330 | 418 | 0.18, 0.12 | 0.99 (77.75%) | 8.97 (22.55%) | 6.76 | 0.09 |
| **1** | 317 (58066), 390 (48085) | 330 | 435 | 0.16, 0.10 | 1.75 (28.12%) | 19.66 (71.88%) | 19.06 | 0.25 |
| **2** | 318 (59580), 387 (32670) | 330 | 428 | 0.16, 0.05 | 2.22 (36.55%) | 19.63 (63.45%) | 18.56 | 0.17 |
| **3** | 323 (54749), 382 (35488) | 330 | 431 | 0.15, 0.09 | 1.25 (62.81%) | 11.28 (37.19%) | 9.70 | 0.11 |
| **4** | 315 (68137), 369 (45865) | 330 | 444 | 0.16, 0.05 | 1.06 (61.32%) | 10.14 (38.68%) | 8.85 | 0.23 |

[a]Recorded in acetonitrile at 298 K, concentration = $10^{-5}$ mol $L^{-1}$; [b]Decay mean lifetime; [c]Quantum efficiency

**Table S8.** Photoluminescent Data for **L** and **1**–**4** in solid state at 298 K

| Compound | Excitation ($\lambda_{ex}$, nm) | Emission ($\lambda_{max}$, nm) | CIE 1931 (x, y) | $\tau_1$ (µs) | $\tau_2$ (µs) | $(\tau, µs)^a$ |
|---|---|---|---|---|---|---|
| **L** | 330 | 470 | 0.16, 0.25 | 1.42 (54.45%) | 13.88 (45.55%) | 12.52 |
| **1** | 330 | 472 | 0.14, 0.24 | 1.75 (43.23%) | 22.16 (56.77%) | 21.00 |
| **2** | 330 | 464 | 0.14, 0.14 | 2.28 (33.50%) | 36.60 (66.50%) | 35.55 |
| **3** | 330 | 470 | 0.13, 0.20 | 2.19 (39.96%) | 30.09 (60.04%) | 28.79 |
| **4** | 330 | 472 | 0.16, 0.25 | 1.70 (52.82%) | 20.30 (47.18%) | 18.71 |

[a]Decay mean lifetime

## REFERENCES

(1) Viswanathan, S.; Bettencourt-Dias, A. Inorg. Chem. 2006, 45, 10138–10146.

(2) Sheldrick, G. M. *SHELXL 97 Program for Crystal Structure Refinement, University of Göttingen, Göttingen, Germany,* **1997**.

(3) Sheldrick, G. M. *SHELXL 97 Program for Crystal Structure Solution, University of Göttingen, Göttingen, Germany,* **1997**.